

International Journal of Data Analysis Techniques and Strategies

ISSN online: 1755-8069 - ISSN print: 1755-8050
<https://www.inderscience.com/ijdats>

Effect of noise uncertainty during spectrum sensing for cognitive radio ad hoc networks

Debabrata Dansana, Prafulla Kumar Behera

DOI: [10.1504/IJDATS.2023.10054582](https://doi.org/10.1504/IJDATS.2023.10054582)

Article History:

Received:	24 September 2022
Last revised:	10 January 2023
Accepted:	07 February 2023
Published online:	28 July 2023

Effect of noise uncertainty during spectrum sensing for cognitive radio ad hoc networks

Debabrata Dansana* and
Prafulla Kumar Behera

Department of Computer Science and Applications,
Utkal University,

Bhubaneswar, Odisha, India

Email: debabratadansana07@gmail.com

Email: p_behera@hotmail.com

*Corresponding author

Abstract: Cognitive radio network is a technique where underutilised licensed spectrum allows opportunistic access to unlicensed secondary users. Different spectrum sensing algorithms are used to sense the presence or absence of primary licensed users in noisy and fading channel. This paper provides a comparative analysis of different spectrum sensing algorithms for cognitive radio network based on dynamic threshold and noise uncertainty. Spectrum sensing in cognitive radio network based on fixed threshold are sensitive to noise, therefore these are not efficient enough. The use of dynamic threshold improves performance of the spectrum detection without much computational complexity. Different computer simulations are provided for the dynamic threshold with and without noise uncertainty for spectrum sensing of cognitive radio network. The performance of the spectrum sensing techniques is evaluated by receiver operating characteristics (ROC) curves over additive white Gaussian noise (AWGN) and different fading channels (Rayleigh and Nakagami-m).

Keywords: spectrum sensing; dynamic threshold; cognitive radio ad hoc network; CRAHN; fading channel; noise uncertainty; receiver operating characteristics; ROC; additive White Gaussian noise; AWGN; signal-to-noise-ratio; SNR.

Reference to this paper should be made as follows: Dansana, D. and Behera, P.K. (2023) 'Effect of noise uncertainty during spectrum sensing for cognitive radio ad hoc networks', *Int. J. Data Analysis Techniques and Strategies*, Vol. 15, Nos. 1/2, pp.41–56.

Biographical notes: Debabrata Dansana is a PhD scholar at Utkal University, Bhubaneswar, Odisha in the Department of Computer Science and Applications. His research focuses on topics such as cognitive radio ad hoc networks, artificial intelligence, machine learning, and related areas. He has a strong publication record, with more than 15 research papers published in various international journals including IEEE, Springer, Frontiers, etc. With his research work, he aims to contribute to the advancement of computer science and its impact on society.

Prafulla Kumar Behera is working as an Associate Professor in Computer Science at Utkal University, Bhubaneswar, Odisha. He received PhD in Computer Science and Applications. He published more than 50 articles in national and international journals. He published more the three authored and edited book. He is passionate about technology and its application in solving real-world problems.

1 Introduction

Spectrum allocation and access is a tightly controlled policy where licensed users are provided exclusive access to the fixed spectrum band. The increasing number of mobile devices causes this demand. The Federal Communications Commission (FCC) anticipated that spectrum authorisations would be used ranging from 15% to 85% of the time (Akyildiz et al., 2009b). On the other hand, licensed spectrum is seldom used (Akyildiz et al., 2009a), which is a direct result of the existing restrictions on spectrum allocation. As a result of poor spectrum usage and rising demand for spectrum, the FCC authorised the opportunistic use of licensed spectrum, which included TV white spaces (Akyildiz et al., 2006). A part of the spectrum that has been licensed has been set aside for the use of TV white spaces. When challenges are handled in such a manner, new network topologies come into being, such as the cognitive radio (CR) network. The CR network is one solution that has been proposed addressing the problem of inefficient spectrum utilisation in wireless ad hoc networks. When there are no primary users around to make use of the licensed spectrum, this form of network makes it possible for secondary users, also known as SUs, to have opportunistic access to it. The CR network overarching objective is to speed up the delivery of data, and one way in which this objective might be met is by the implementation of a routing protocol. The decisions that are taken by prime users (PUs) (Chandrashekar and Lazos, 2010) have a significant impact on the transmissions of secondary users. If a PU appears on a channel, an SU will instantly change to a different channel or choose a new route in order to continue transmitting data. This is done in order to avoid being disrupted by the PU. In the event that another channel is not available, the SU will utilise the routing protocol to choose a new route; if this is not possible, it will switch channels. When there is an issue with the connection, the rerouting process takes much more time than normal. In order to lessen the impact of this challenge, we devised a routing system that, in the event that a connection is lost, would suggest trying one of many other routes. Statistical analysis reveals that a significant amount of licensed spectrum is severely underutilised in the temporal as well as spatial domains. The unused spectrum bands are termed ‘spectrum holes’. Dynamic spectrum access (DSA) is a technique that allows secondary users to access the spectrum holes in a licensed channel using IEEE SCC 41, ETSI, and ITU-R. DSA improves the utilisation of licensed spectrum (Song et al., 2012; Yin et al., 2012). Using DSA, secondary users dynamically search for spectrum holes and temporarily access the wireless communication channel. The ability to detect the availability of licensed spectrum, flexibility to adjust the operating frequency, and opportunistically access the licensed spectrum has provided widespread acceptance to software defined radio (SDR) (Farrell et al., 2009) and CR (Mitola and Maguire, 1999; Haykin, 2005; Zeng et al., 2010; Nguyen et al., 2012; Wang et al., 2011). Technical (hardware and software as well as standard aspects), network policy, and network security-related issue (Clancy and Goergen, 2008; Hlavacek and Chang, 2014; Elakashlan et al., 2014) of CR has been the main area of research. An energy-efficient based routing system (Kalra et al., 2022) has been proposed for mobile ad hoc networks; however, it cannot be used in CRN networks due to its lack of compatibility. The authors’ cross-layer routing algorithm, which is detailed in Naveen Raj et al. (2020), operates on the assumption that the positions and activities of PUs are already known in advance. As a result of the fact that the sharing of information is prohibited by the basic principles of CRN, doing this is a breach of those regulations. An infrastructure-based spectrum-aware routing strategy was developed by

Wang et al. for CRNs (Wang et al., 2017). The protocol may determine the optimum route selection for each node in the network based on aggregated data from the network; however, it cannot be used to CR ad hoc networks since it is not compatible with such networks. Using a number of different factors, a number of research articles (Raj et al., 2020; Sethi and Pal, 2014; Ali et al., 2011) were read in order to determine the optimal approach. In order to arrive at these figures, a lot of different factors, such as the channel latency, the availability of channels, and the probability of PU interference, are taken into consideration. It is possible for the protocol to be unsuccessful if CRN's behaviour deviates from what is assumed in it. A metric-based routing system is suggested as a potential solution in Abdelaziz and ElNainay (2014), which can be found here. If you want this procedure to be successful, you have to make certain that the following conditions are met: This involves having PUs that are constantly on, having exact knowledge of where PUs are located, and having a statistical comprehension of the channels that are accessible. These theories are invalidated by the behaviours shown by the CRN node. IEEE 802.22 Software Group (WG) was formed to define a standardised air interface based on CRs. The IEEE 802.22 standard for wireless regional area networks requires that CR nodes sense the spectrum to detect the presence or absence of active primary transmitters. CR comprises of analog RF front-end and a processor [digital signal processor (DSP), field programmable gate array (FPGA), and general purpose processor] (Shabara et al., 2017).

The selection of threshold λ_e for spectrum sensing in CR network is made by three different approaches such as:

- constant false alarm rate (CFAR): PRE-defined value of false alarm probability
- constant detection rate (CDR): fixing detection probability
- minimised error probability (MEP): minimising error probability and differentiating with respect to the threshold.

Uncertainty in signal and noise limits the performance of the CR spectrum sensing detector. Uncertainty can creep into the system from intentional under-modelling, calculated noise from the sources and environment, etc. Excellent literature on mathematical modelling of noise uncertainty can be found in Tandra and Sahai (2008), whereas in Lopez-Benitez and Casadevall (2013), the authors have modelled the signal uncertainty in the CR network. As the real world is never perfect, the uncertainty condition must be considered during the design of the detector.

In opportunistic spectrum access, performance failure of spectrum sensing has a catastrophic effect on the primary user. It creates harmful interference on the primary user, not undesirable. The main objective of this research is to ascertain the performance of a detection scheme that scans the spectrum and finds the presence of any primary user. This paper provides a detailed analysis of spectrum sensing techniques of the CR network. Different spectrum sensing techniques such as matched filter detection, energy detector, and cyclostationary feature detection are evaluated. The noise and dynamic threshold issues in CR networks have been discussed in detail. Uncertainty of noise and dynamic threshold of CR has been simulated using MATLAB.

The performance of spectrum sensing techniques under different fading channels, such as Rayleigh and Nakagami-B, the performance of spectrum sensing under different thresholds, and the performance of spectrum sensing considering noise uncertainty have

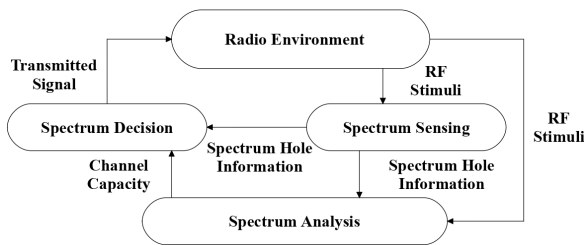
been mathematically formulated and discussed. This paper comprises different sections. Section 2 provides a detailed analysis of spectrum sensing in CR, such as matched filter detection, energy detection, and cyclostationary feature detection. Section 3 provides results and discussion for CR spectrum sensing with dynamic threshold and noise uncertainty. This article comes to close with the conclusion and future scope in Section 4.

2 Spectrum sensing in CR

Figure 1 illustrates the cognitive cycle of the CR network. There are three main functions of the cognitive cycle such as:

- a spectrum sensing
- b spectrum decision
- c spectrum analysis (Gupta and Kumar, 2019).

Figure 1 Cognitive cycle of CR network



The CR network operates in two distinct modes: non-interfering mode and interfering tolerant mode. In non-interfering mode, there is no interference to the primary spectrum. The secondary users of the CR network exploit only the white spaces of the primary system. In non-interfering mode, quality of service (QoS) is not compromised.

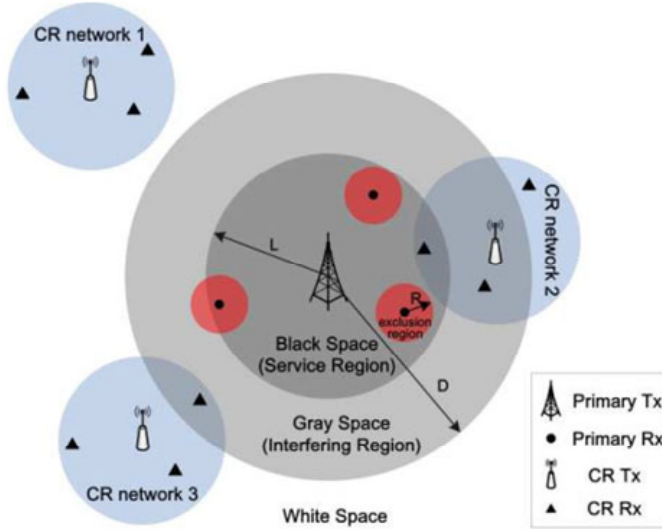
Figure 2 illustrates the coexistence of the primary and randomly distributed CR networks.

The binary hypothesis testing problem for spectrum sensing can be represented as:

$$\begin{cases} H_0 : Y(n) = W(n) \quad n = 1, 2, \dots, N \\ H_1 : Y(n) = X(n) + W(n) \quad n = 1, 2, \dots, N \end{cases} \quad (1)$$

where $Y(n)$ is the received signal at the CR node, $X(n)$ is the transmitted signal at primary nodes, and $W(n)$ is the white noise samples, respectively. Noise samples are from the white Gaussian noise process with spectral density σ_n^2 , i.e., $W(n) \sim N(0, \sigma_n^2)$. The statistics are entirely known to the receiver. H_0 signifies that the licensed user is absent and the channel is vacant, H_1 signifies that the licensed user is present and the track is occupied

Figure 2 Coexistence of primary network and randomly distributed CR network (see online version for colours)



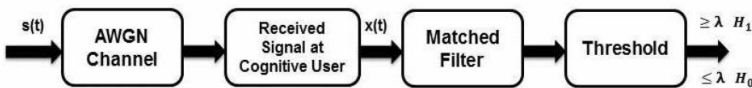
Three essential metrics are $-P_d$ is probability detection when the channel is vacant and declared as vacant, P_f is the probability of a false alarm when a channel is vacant and declared as occupied, and P_m is the probability of miss detection when the channel is occupied and declared as vacant.

A detailed review of spectrum sensing in CR networks has been discussed in Yucek and Arslan (2009). Table 1 illustrate the comparative analysis among different spectrum sensing techniques. Spectrum sensing can be categorised as transmitter detection, cooperative detection and interference temperature detection. Transmitter detection can also be categorised as matched filter detection, energy detection and cyclostationary detection. Dynamic threshold energy detection has been discussed in Yu et al. (2009).

2.1 Matched filter detection

Matched filter is a linear filter, and it enlarges signal-to-noise-ratio (SNR) of PU signal at the CR user terminal under AWGN channel. It matched filter detection based on the principle of coherent detection. Figure 3 illustrates the block diagram of match filter detection.

Figure 3 Matched filter detection



The matched filter can be represented as

$$D(Y) = \frac{1}{N} \sum_{n=0}^{N-1} Y(n)X(n) \tag{2}$$

where $D(Y)$ is the decision variable, γ is the decision threshold, N is the number of samples.

If the noise variance is completely known, then according to the central limit theorem.

$$\begin{aligned} D(Y) &> \gamma H_1 \\ D(Y) &< \gamma H_0 \end{aligned} \tag{3}$$

The equation for P_d , P_f , and P_m for the matched filter is derived as:

$$P_d = P_r \left(D(x) > \frac{\lambda}{H_1} \right) = Q \left(\frac{\lambda - P}{\sqrt{\frac{P\sigma_n^2}{N}}} \right) \tag{4}$$

$$P_f = P_r \left(D(x) > \frac{\lambda}{H_0} \right) = Q \left(\frac{\lambda - P}{\sqrt{\frac{P\sigma_n^2}{N}}} \right) \tag{5}$$

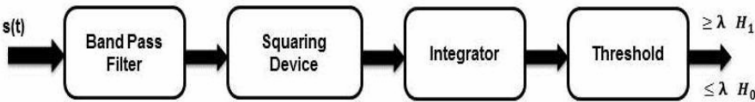
$$P_m = 1 - P_d = 1 - Q \left(\frac{\lambda - P}{\sqrt{\frac{P\sigma_n^2}{N}}} \right) \tag{6}$$

When sufficient information regarding the primary user signal is unavailable, matched filter detection can not be used.

2.2 Energy detection

The mathematical modelling of energy detection is discussed in Umar et al. (2013). Figure 4 illustrates the block diagram of energy detection comprised of a bandpass filter (BPF), squaring unit integrator unit, and threshold unit. The sensing time of the energy detector is higher, and it cannot discriminate between the PU signal and cognitive user signal.

Figure 4 Block diagram of energy detection



The equations for P_d , P_f , and P_m for energy detection are derived as:

$$P_d = P_r \left(D(x) > \frac{\lambda}{H_1} \right) = Q \left(\frac{\lambda - (P + \sigma_n^2)}{\sqrt{\frac{2}{N} (P + \sigma_n^2)}} \right) \tag{7}$$

$$P_f = P_r \left(D(x) > \frac{\lambda}{H_0} \right) = Q \left(\frac{\lambda - \sigma_n^2}{\sqrt{\frac{2}{N} (\sigma_n^2)}} \right) \tag{8}$$

$$P_m = 1 - P_d = 1 - Q\left(\frac{\lambda - (P + \sigma_n^2)}{\sqrt{\frac{2}{N}}(P + \sigma_n^2)}\right) \quad (9)$$

where $Q(\cdot)$ function represents the complementary cumulative distribution of the standard Gaussian function and λ represents the pre-set threshold value.

2.3 Cyclostationary feature detection

Most of the signals in the communication system can be modelled as cyclostationary by nature because it exhibits different statistical attributes such as mean, auto-correlation, etc. These statistical attributes are time-varying in nature. In cyclostationary feature detection, cyclostationary features are used to detect the presence or absence of a signal. Figure 5 illustrates the block diagram of cyclostationary feature detection.

Figure 5 Block diagram of cyclostationary feature detection



The equations for P_d , P_f , and P_m for cyclostationary feature detection are derived as

$$P_d = P_r\left(D(x) > \frac{\lambda}{H_1}\right) = Q\left(\sqrt{\frac{2SNR}{\sigma_n^2}}, \frac{\lambda}{\sigma_A}\right) \quad (10)$$

$$P_f = P_r\left(D(x) > \frac{\lambda}{H_0}\right) = e^{-\frac{\lambda^2}{2\sigma_A^2}} \quad (11)$$

$$P_m = 1 - P_d = 1 - Q\left(\sqrt{\frac{2SNR}{\sigma_n^2}}, \frac{\lambda}{\sigma_A}\right) \quad (12)$$

where $SNR = \frac{P}{\sigma_n^2}$ and $\sigma_A^2 = \frac{\sigma_n^2}{2N+1}$.

Table 1 Comparison of different spectrum sensing techniques

Type	Energy detection	Matched filter	Cyclostationary
Sensing time	More	Less	Most
Implementation	Simple	Complex	Complex
Performance under noise	Poor	Bad	Good
Prior knowledge required	No	Yes	No

2.4 Performance analysis under fading channel

The average detection probability P_d over any fading channel is computed by averaging the detection probability over all SNR, as shown.

$$P_d = \int_0^{\infty} P_d(\gamma, \lambda) f(\gamma) d\gamma \quad (13)$$

where $f(\gamma)$ is the SNR distribution of fading channel, and $P_d(\gamma, \lambda)$ is the detection probability.

2.4.1 Rayleigh fading channel

Rayleigh fading channel occurs when there is no such dominant path between the primary user and secondary user, and the receiving signal amplitude at the secondary user follows Rayleigh distribution. SNR distribution for the Rayleigh fading channel is represented as:

$$f_{ray}(\gamma) = \frac{1}{\gamma} e^{-\left(\frac{\gamma}{\bar{\gamma}}\right)} \quad (14)$$

The probability of Rayleigh fading channel is represented as:

$$P_d^{rayleigh} = 1 - \frac{1}{2} \left[\operatorname{Erfc} \left(\frac{N\sigma_n^2 - \lambda}{\sqrt{2N}\sigma_n^2} \right) - \left(e^{\left(\frac{1}{\gamma^2} + \frac{4(N\sigma_n^2 - \lambda)}{\gamma \sqrt{2N}\sigma_n^2} \right) \frac{\sqrt{N}}{2}} \operatorname{Erfc} \left(\frac{N\sigma_n^2 - \lambda}{\sqrt{2N}\sigma_n^2} + \frac{1}{\bar{\gamma} \sqrt{2N}} \right) \right) \right] \quad (15)$$

where Erfc is the complementary error function.

2.4.2 Nakagami- m fading channel

Nakagami- m fading channel is a multipath fading channel that depends on shape parameter m . SNR distribution of the Nakagami- m fading channel is represented as:

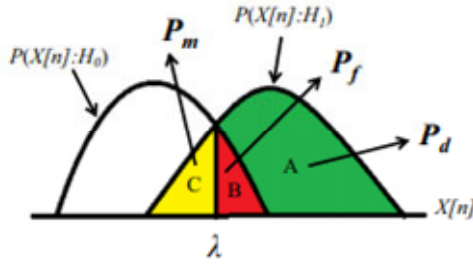
$$f_{naka}(X) = \frac{\left(\frac{m}{\gamma}\right)^m}{\tau(m)} (x^{m-1}) e^{-\left(\frac{mx}{\gamma}\right)} \quad (16)$$

The probability of Nakagami- m fading channel is represented as:

$$P_d^{Naka} = 1 - \frac{\left(\frac{m}{\gamma}\right)^m}{2\tau(m)} \int_0^{\infty} (x^{m-1}) e^{-\left(\frac{mx}{\gamma}\right)} \operatorname{Erfc} \left(\sqrt{\frac{N}{2}} x + \frac{N\sigma_n^2 - \lambda}{\sqrt{2N}\sigma_n^2} \right) \quad (17)$$

2.5 Selection of threshold

Figure 6 shows that the threshold selection is optimal when the threshold is selected as intersection between PDF of H_0 and H_1 .

Figure 6 Threshold selection with hypothesis model (see online version for colours)

Fixed threshold calculation using CFAR and CDR can be computed as:

$$\begin{aligned}\lambda_{CFAR} &= \sigma_n^2 \left(L + Q^{-1} P_f 2L \right) \\ \lambda_{CDR} &= \sigma_i^2 \left(L + Q P_d \sqrt{2L} \right)\end{aligned}\quad (18)$$

In a fixed threshold, there is a constant in the received SNR. Due to the limitation of a fixed threshold, the dynamic threshold is considered. To compute dynamic threshold, $\frac{\partial P_e}{\partial \lambda} = 0$. Apart from the fixed and dynamic threshold, Neyman-Pearson (NP) approach and Bayesian detector (BD) approach also has been used. The value of threshold using NP can be computed as:

$$\lambda_{NP} = 2 \left(\frac{\ln \lambda - \frac{L}{2} \ln \left(\frac{\sigma_n^2}{\sigma_i^2} \right)}{\sigma_s^2} \right) \sigma_n^2 \sigma_i^2 \quad (19)$$

The value of the threshold using the BD approach can be computed as:

$$\lambda_{BD} = 2 \left(\frac{\ln \left(\frac{P(H_0)}{P(H_1)} \right) - \frac{L}{2} \ln \left(\frac{\sigma_n^2}{\sigma_i^2} \right)}{\sigma_s^2} \right) \sigma_n^2 \sigma_i^2 \quad (20)$$

The selection of the threshold for MEP in the AWGN channel is given as:

$$\lambda_e = \left(1 + \sqrt{1 + \frac{2 + (2 + \lambda) \ln(1 + \lambda)}{N_\lambda}} \right) \left(\frac{1 + \lambda}{1 + \frac{\lambda}{2}} \right) \frac{N \sigma_n^2}{2} \quad (21)$$

For the Rayleigh channel, the selection of threshold can be provided as:

$$\lambda_e = \left(1 + \sqrt{\frac{2}{N}} + \sqrt{\frac{2}{N_\pi}} + \sqrt{\frac{2}{N} \left(\frac{1}{\pi} + \sqrt{\frac{2}{N_\pi} \bar{\lambda} - 1} \right)} \right) N \sigma_n^2 \quad (22)$$

For Nakagami-m fading channel, the selection of threshold can be provided as:

$$\lambda_e = \left(1 + \frac{2}{N_{\bar{\lambda}}} - \frac{1}{2\sqrt{2N}} (\sqrt{\pi} - \sqrt{\pi - 8 + 2N\bar{\lambda}^2}) \right) N\sigma_n^2 \quad (23)$$

2.6 Effect of noise uncertainty

For making spectrum sensing in CR robust, the noise uncertainty ρ is considered where $\rho \geq 1$.

If $\rho = 1$, there is no fluctuation in noise power. N can be expressed in terms of noise uncertainty ρ as:

$$N = \frac{2 \left[\rho Q^{-1} P_f - \left(\frac{1}{\rho} + SNR \right) Q^{-1} P_d \right]}{\left[SNR - \left(\rho - \frac{1}{\rho} \right) \right]^2} \quad (24)$$

3 Result and discussion

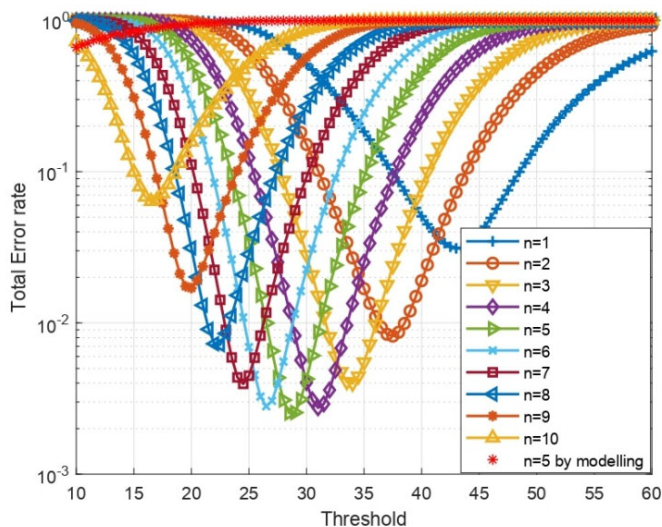
In this simulation the performance of the spectrum sensing techniques is evaluated by receiver operating characteristics (ROC) curves over additive White Gaussian noise (AWGN) and different fading channels (Rayleigh and Nakagami-m). The simulations were carried out in four different scenarios, i.e., fixed SNR, variable SNR, fixed N , and variable N . Initially collects large-scale network and node information sets, and uses them for the analysis of threshold, total error rate, energy detection. To prove the superiority of the algorithm in low SNR plots between P_d and P_{fa} called region ROC curves are plotted. With the theoretical analysis of matched filter detection, energy detection, and cyclostationary detection, MATLAB-based implementation is performed to verify the theoretical credentials.

Figure 7(a) provides the total error rate v/s threshold for CR networks where ten numbers of nodes are taken which are represented as $n = 1$ to $n = 10$, from this figure it can be observed that as threshold value increases, the error rate decreases. Figure 7(b) provides the number of users' v/s threshold for CR users. For SNR = 10 dB, the threshold value is around 27; for SNR = -10 dB, the threshold is 38, which shows the relation between SNR and threshold from the perspective of a number of users.

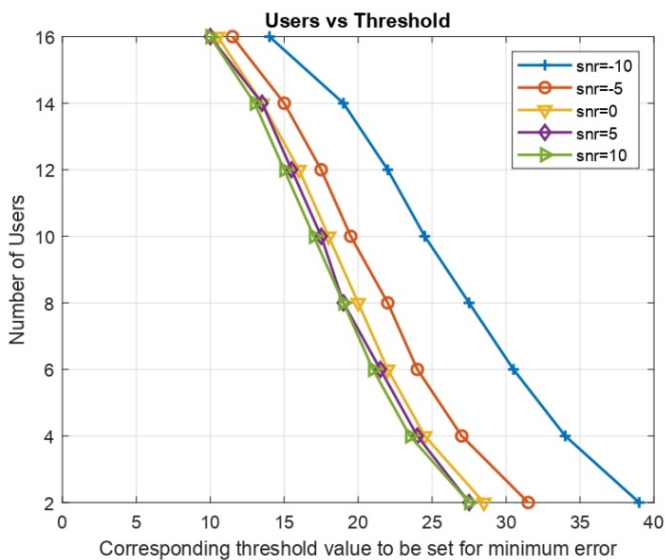
To study the effect of noise uncertainty in spectrum sensing of CR network, it is assumed that the noise is AWGN with zero mean and variance with a noise uncertainty factor ranging between 1 to 1.06 and SNR between -10 dB to -20 dB with $N = 500$ –1,500. Figure 8 shows the PD v/s SNR for a fixed threshold value in a CR network. Figure 8 shows that the SNR value increases with an increase in the PD value (P_d); thus, to get accurate results in energy detection, the SNR value must be as high as possible.

Figure 9(a) represents the plot between probability of false alarm (P_{FA}) and the P_D thresholds using no noise uncertainty, with noise uncertainty, dynamic threshold both noise uncertainty and dynamic threshold, it can be observed that despite of low value of SNR, spectrum sensing performs better in dynamic threshold conditions under pre-defined performance metrics.

Figure 7 (a) Total error rate v/s threshold and (b) Number of users v/s threshold (see online version for colours)



(a)



(b)

Figure 9(b) illustrates the ROC curve between P_f and P_d with SNR = -15 dB, $N = 1,500$, and difference values noise uncertainty ρ , the ROC curve for different noise uncertainty N and at a fixed SNR value of -15 dB and $N = 1,500$, the ROC curves for comparing the detection performance without and with noise uncertainty for different values of noise uncertainty coefficient values (i.e., 1.01, 1.03 and 1.05), SNR = -15 dB and $N = 1,500$. From the plot it is found that without noise PD is very sensitive to noise uncertainty where the performance gradually reduces as the noise factor increases.

Figure 8 Probability of detection (P_D) v/s SNR for a fixed threshold

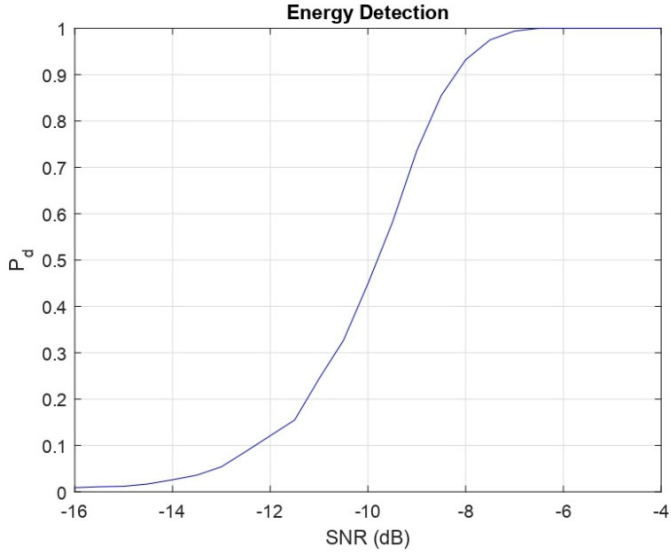
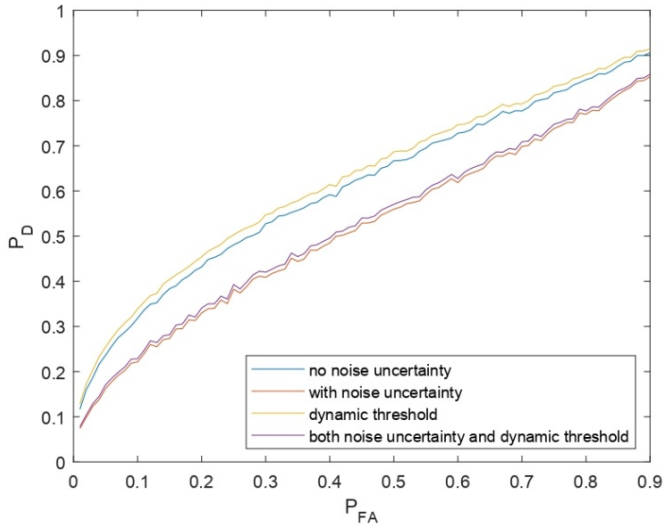
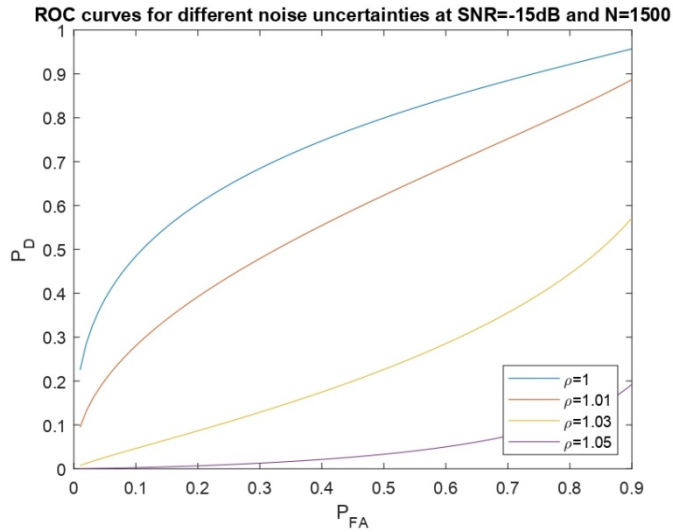


Figure 9 P_{FA} v/s P_D ROC for (a) noise uncertainty and dynamic threshold, (b) noise uncertainty at SNR = -15 dB and $N = 1,500$, (c) different SNR at $N = 500$, (d) different N at SNR = -15 dB (see online version for colours)

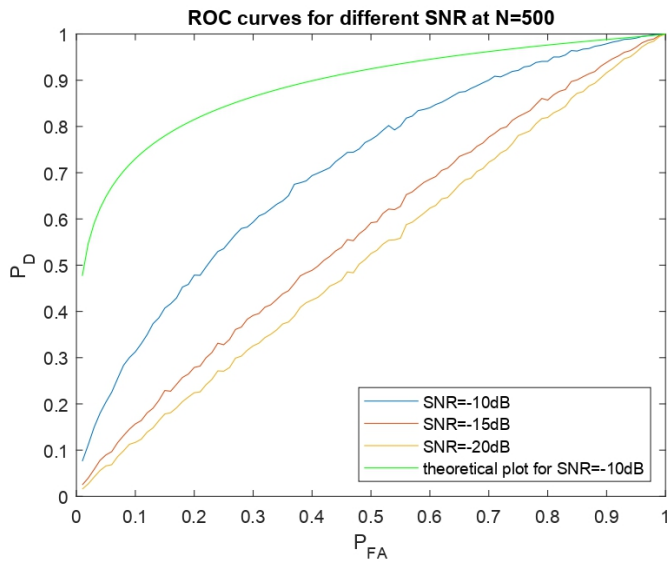


(a)

Figure 9 PFA v/s PD ROC for (a) noise uncertainty and dynamic threshold, (b) noise uncertainty at SNR = -15 dB and $N = 1,500$, (c) different SNR at $N = 500$, (d) different N at SNR = -15 dB (continued) (see online version for colours)



(b)



(c)

Figure 9 PFA v/s PD ROC for (a) noise uncertainty and dynamic threshold, (b) noise uncertainty at SNR = -15 dB and $N = 1,500$, (c) different SNR at $N = 500$, (d) different N at SNR = -15 dB (continued) (see online version for colours)

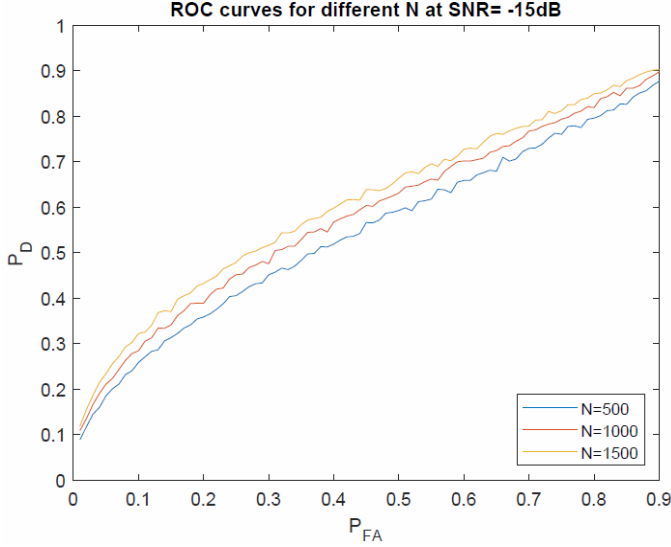


Figure 9(c) represents the ROC curve for the value of SNR at a fixed N of 500, the plot represent relationship between P_{FA} and the P_D thresholds using noise uncertainty and dynamic thresholds for -20 dB to -10 dB average SNR, sample size $N = 500$. From this plot it can be observed that with increasing SNR, the PD rises rapidly. Figure 9(d) illustrates the ROC curve for different values of N at SNR = -15 db.

From the simulation results, which has been carried out on different scenarios such as fixed SNR, variable SNR, fixed N , and variable N , it can be concluded that despite of low value of SNR, the spectrum sensing performs better in dynamic threshold condition under a pre-defined performance metrics.

4 Conclusions and future scope

This paper provides a detailed comparative analysis of different spectrum sensing techniques. Different performance metrics for spectrum sensing have been evaluated for all the techniques. Three different channels, such as AWGN, Rayleigh, and Nakagami-m fading channels, have been considered, and performance metrics for each of the scenario has been computed. Noise uncertainty has been considered for the CR network, and the PD under noise uncertainty has been evaluated for all the scenarios. MATLAB-based simulations provide the ROC of different probabilistic matrices for CR networks under different fading channels and under noise uncertainty conditions in dynamic threshold conditions. From the various simulations carried out, it can be proved that the dynamic threshold performs better in spectrum sensing of CR under noise uncertainty. In the future, these techniques needs to be validated on many communication nodes and channels. This performance can also be improved through the proper selection of routes.

As cognitive radio ad hoc networks (CRAHNs) use DSA techniques, the network security-related CR has been the main area of research that plays a vital role in communication. In the future, utilising a variety of security models can help with incremental efficiency optimisation under various attack types.

References

- Abdelaziz, S. and ElNainay, M. (2014) 'Metric-based taxonomy of routing protocols for cognitive radio ad hoc networks', in *Journal of Network and Computer Applications*, Vol. 40, pp.151–163, Elsevier BV, <https://doi.org/10.1016/j.jnca.2013.09.001>.
- Akyildiz, I.F., Lee, W.Y., Vuran, M.C. and Mohanty, S. (2006) 'NeXt generation/dynamic spectrum access/cognitive radio wireless networks: a survey', *Computer Networks Journal*, Sept., Vol. 50, No. 13, pp.2127–2159, Elsevier BV, <https://doi.org/10.1016/j.comnet.2006.05.001>.
- Akyildiz, I.F., Lee, W.Y. and Chowdhury, K.R. (2009a) 'Spectrum management in cognitive radio ad hoc networks', *IEEE Networks Magazine-Special Issue on Networking over Multi-Hop Cognitive Networks*, to appear.
- Akyildiz, I.F., Lee, W-Y. and Chowdhury, K.R. (2009b) 'CRAHNs: cognitive radio ad hoc networks', in *Ad Hoc Networks*, Vol. 7, No. 5, pp.810–836, Elsevier BV, <https://doi.org/10.1016/j.adhoc.2009.01.001>.
- Ali, A., Iqbal, M., Baig, A. and Wang, X. (2011) 'Routing techniques in cognitive radio networks: a survey', *International Journal of Wireless & Mobile Networks*, Vol. 3, No. 3, pp.96–110.
- Chandrashekar, S. and Lazos, L. (2010) 'A primary user authentication system for mobile cognitive radio networks', *2010 3rd International Symposium on Applied Sciences in Biomedical and Communication Technologies (ISABEL)*, 7–10 Nov., pp.1–5.
- Clancy, T.C. and Goergen, N. (2008) 'Security in cognitive radio networks: threats and mitigation', in *2008 3rd International Conference on Cognitive Radio Oriented Wireless Networks and Communications (CrownCom 2008)*, IEEE, pp.1–8.
- Elkashlan, M., Wang, L., Duong, T.Q., Karagiannidis, G.K. and Nallanathan, A. (2014) 'On the security of cognitive radio networks', *IEEE Transactions on Vehicular Technology*, Vol. 64, No. 8, pp.3790–3795.
- Farrell, R., Sanchez, M. and Corley, G. (2009) 'Software-defined radio demonstrators: an example and future trends', *International Journal of Digital Multimedia Broadcasting*, Vol. 2009, pp.1–12, Hindawi Limited, <https://doi.org/10.1155/2009/547650>.
- Gupta, M.S. and Kumar, K. (2019) 'Progression on spectrum sensing for cognitive radio networks: a survey, classification, challenges and future research issues', in *Journal of Network and Computer Applications*, Vol. 143, pp.47–76, Elsevier BV, <https://doi.org/10.1016/j.jnca.2019.06.005>.
- Haykin, S. (2005) 'Cognitive radio: brain-empowered wireless communications', *IEEE Journal on Selected Areas in Communications*, Vol. 23, No. 2, pp.201–220.
- Hlavacek, D. and Chang, J.M. (2014) 'A layered approach to cognitive radio network security: a survey', *Computer Networks*, Vol. 75, pp.414–436, Elsevier BV, <https://doi.org/10.1016/j.comnet.2014.10.001>.
- Kalra, M., Vohra, A. and Marriwala, N. (2022) 'LEACH based hybrid energy efficient routing algorithm for dynamic cognitive radio networks', in *Measurement: Sensors*, Vol. 24, p.100419, Elsevier BV, <https://doi.org/10.1016/j.measen.2022.100419>.
- Lopez-Benitez, M. and Casadevall, F. (2013) 'Signal uncertainty in spectrum sensing for cognitive radio', *IEEE Transactions on Communications*, Vol. 61, No. 4, pp.1231–1241.
- Mitola, J. and Maguire, G.Q. (1999) 'Cognitive radio: making software radios more personal', *IEEE Personal Communications*, Vol. 6, No. 4, pp.13–18.

- Naveen Raj, R., Nayak, A. and Kumar, M.S. (2020) 'Spectrum-aware cross-layered routing protocol for cognitive radio ad hoc networks', in *Computer Communications*, Vol. 164, pp.249–260, Elsevier BV, <https://doi.org/10.1016/j.comcom.2020.10.011>.
- Nguyen, V.T., Villain, F. and Le Guillou, Y. (2012) 'Cognitive radio rf: overview and challenges', *VLSI Design*, Vol. 2012, pp.1–13, Hindawi Limited, <https://doi.org/10.1155/2012/716476>.
- Raj, R.N. et al (2020) 'Spectrum-aware cross-layered routing protocol for cognitive radio ad hoc networks', *Computer Communications*, 1 December, Vol. 164, pp.249–260, Elsevier BV, <https://doi.org/10.1016/j.comcom.2020.10.011>.
- Sethi, S. and Pal, S. (2014) 'Effective routing protocol in cognitive radio ad hoc network using fuzzy-based reliable communication neighbor node selection', in Satapathy, S., Udgata, S. and Biswal, B. (Eds.): *Proceedings of the International Conference on Frontiers of Intelligent Computing: Theory and Applications (FICTA) 2013. Advances in Intelligent Systems and Computing*, Vol. 247, Springer, Cham, https://doi.org/10.1007/978-3-319-02931-3_3.
- Shabara, Y., Mohamed, A. and Al-Ali, A.K. (2017) 'A hardware implementation for efficient spectrum access in cognitive radio networks', in *2017 IEEE Wireless Communications and Networking Conference (WCNC)*, IEEE, pp.1–6.
- Song, M., Xin, C., Zhao, Y. and Cheng, X. (2012) 'Dynamic spectrum access: from cognitive radio to network radio', *IEEE Wireless Communications*, Vol. 19, No. 1, pp.23–29.
- Tandra, R. and Sahai, A. (2008) 'SNR walls for signal detection', *IEEE Journal of Selected Topics in Signal Processing*, Vol. 2, No. 1, pp.4–17.
- Umar, R., Sheikh, A.U. and Deriche, M. (2013) 'Unveiling the hidden assumptions of energy detector based spectrum sensing for cognitive radios', *IEEE Communications Surveys & Tutorials*, Vol. 16, No. 2, pp.713–728.
- Wang, J., Ghosh, M. and Challapali, K. (2011) 'Emerging cognitive radio applications: a survey', *IEEE Communications Magazine*, Vol. 49, No. 3, pp.74–81.
- Wang, J., Yue, H., Hai, L. and Fang, Y. (2017) 'Spectrum-aware anypath routing in multi-hop cognitive radio networks', in *IEEE Transactions on Mobile Computing*, Vol. 16, No. 4, pp.1176–1187, Institute of Electrical and Electronics Engineers (IEEE) <https://doi.org/10.1109/tmc.2016.2582173>.
- Yin, S., Chen, D., Zhang, Q., Liu, M. and Li, S. (2012) 'Mining spectrum usage data: a large-scale spectrum measurement study', *IEEE Transactions on Mobile Computing*, Vol. 11, No. 6, pp.1033–1046.
- Yu, G-C., Shao, Y-B., Long, H. and Yue, G-X. (2009) 'Dynamic threshold based spectrum detection in cognitive radio systems', in *2009 5th International Conference on Wireless Communications, Networking and Mobile Computing*, IEEE, pp.1–4.
- Yucek, T. and Arslan, H. (2009) 'A survey of spectrum sensing algorithms for cognitive radio applications', *IEEE Communications Surveys & Tutorials*, Vol. 11, No. 1, pp.116–130.
- Zeng, Y., Liang, Y-C., Hoang, A.T. and Zhang, R. (2010) 'A review on spectrum sensing for cognitive radio: challenges and solutions', *EURASIP Journal on Advances in Signal Processing*, Vol. 2010, No. 1, pp.1–15, Springer Science and Business Media LLC, <https://doi.org/10.1155/2010/381465>.